Title
Hydrogen peroxide and methylhydroperoxide distributions related to ozone and odd hydrogen over the North Pacific in the fall of 1991

Journal
Journal of Geophysical Research, 101(D1)

ISSN
0148-0227

Authors
Heikes, Brian G
Lee, Meehye
Bradshaw, J
et al.

Publication Date
1996-01-20

DOI
10.1029/95jd01364

JOURNAL OF GEOPHYSICAL RESEARCH, VOL. 101, NO. D1, PAGES 1891–1905, JANUARY 20, 1996

Hydrogen peroxide and methylhydroperoxide distributions related to ozone and odd hydrogen over the North Pacific in the fall of 1991

Brian G. Heikes,[1] Meehye Lee,[1] J. Bradshaw,[2] S. Sandholm,[2] D. D. Davis,[2] J. Crawford,[2] Jose Rodriguez,[3] S. Liu,[4] S. McKeen,[5] D. Thornton,[6] A. Bandy,[6] G. Gregory,[7] R. Talbot,[8] and D. Blake[9]

Abstract. Hydrogen peroxide and methylhydroperoxide were measured in the troposphere over the western North Pacific as part of the airborne portion of NASA's Global Tropospheric Experiment/Pacific Exploratory Mission-West A field mission. The flights circled the North Pacific, focusing on the western Pacific, and extended from 300 to 13,000 m altitude. The hydroperoxides were uniquely separated and quantified using a high-pressure liquid chromatography system in conjunction with a continuous enzyme fluorometric instrument. Results show a latitudinal gradient in both peroxides at all altitudes; for example, between 3 and 5 km, H_2O_2 median values decrease from 1700 to 500 parts per trillion by volume (pptv) in going from 0°–15°N to 45°–60°N, and the corresponding decrease in CH_3OOH was 1100 to 200 pptv. Concentration maxima are observed in both species at altitudes of 2 to 3 km with H_2O_2 concentrations below 1 km lower by 30%, 10% for CH_3OOH, and even lower, by a factor of 10, for both above 9 km. The H_2O_2 to CH_3OOH ratio increased with altitude and latitude with ratios <1 in the tropical surface layer and >2 at midlatitude high altitude. Highest peroxide concentrations were encountered over the Celebes Sea in air which was impacted by aged biomass fire and urban pollutants. CH_3OOH was below the level of detection in stratospheric air. H_2O_2 exceeded SO_2 95% of the time, with the exceptions generally above 9 km. Above 3 km, O_3 increases with decreasing H_2O_2 and CH_3OOH. Below 3 km the O_3-CH_3OOH trend is the same but O_3 increases with increasing H_2O_2. The measurements are compared with predictions based upon a photochemical steady state zero-dimensional model and a three-dimensional mesoscale time-dependent model. These models capture observed trends in H_2O_2 and CH_3OOH, with the possible exception of H_2O_2 below 2 km where surface removal is important. A surface removal lifetime of 3.5 days brings the observed and zero-dimensional model-estimated H_2O_2 into agreement. The steady state model suggests a strong correlation between the ratios of NO/CO or HO_2/HO and the ratio of H_2O_2/CH_3OOH. The observed hydroperoxide ratios bracket the modeled relationship with occasionally much lower H_2O_2 than expected.

Introduction

Hydrogen peroxide (H_2O_2) and methylhydroperoxide (CH_3OOH) measurements were made from the NASA DC-8 aircraft throughout the western Pacific in the fall of 1991. These measurements were part of the suite of gas and aerosol chemical measurements which comprised the NASA Global Tropospheric Experiment/Pacific Exploratory Mission-West A (GTE/PEM-West A), which was a component of the IGAC-APARE program. The NASA GTE scientific program and the PEM-West A experiment are described in detail by *Hoell et al.* [this issue]. In summary, the goals of the mission were twofold: (1) to improve our knowledge of tropospheric ozone over the western Pacific Ocean through an exploration of atmospheric composition and dynamics and (2) to elucidate the chemistry of sulfur gases in this region. The meteorological overview for the experiment is presented by *Bachmeier et al.* [this issue] and the encountered synoptic conditions and transport paths were considered typical for this region in this season [*Merrill*, this issue]. A total of 18 research flights circling the North Pacific were conducted, spanning 0° to 65°N latitude, 115°E to 125°W longitude, and 0 to 13 km altitude. The flights were out of Ames Research Center (4), Anchorage (1), Tokyo (5), Okinawa (1), Hong Kong (3), Guam (4), Wake Island (1), and Honolulu (2). A map of the study area and flight footprints are shown in Figure 1 and detailed by *Hoell et al.* [this issue].

The hydroperoxides are linked to the chemistry of O_3 through peroxyl radicals, HO_2, or CH_3OO [e.g., *Leighton*,

[1]Center for Atmospheric Chemistry Studies, Graduate School of Oceanography, University of Rhode Island, Narragansett.
[2]Georgia Institute of Technology, Atlanta.
[3]AER Incorporated, Cambridge, Massachusetts.
[4]NOAA Aeronomy Laboratory, Boulder, Colorado.
[5]NOAA Cooperative Institute for Research in Environmental Sciences, Boulder, Colorado.
[6]Drexel University, Philadelphia, Pennsylvania.
[7]NASA Langley Research Center, Hampton, Virginia.
[8]Institute for the Study of Earth, Oceans, and Space, University of New Hampshire, Durham.
[9]University of California, Irvine.

Paper number 95JD01364.
0148-0227/96/95JD-01364$05.00

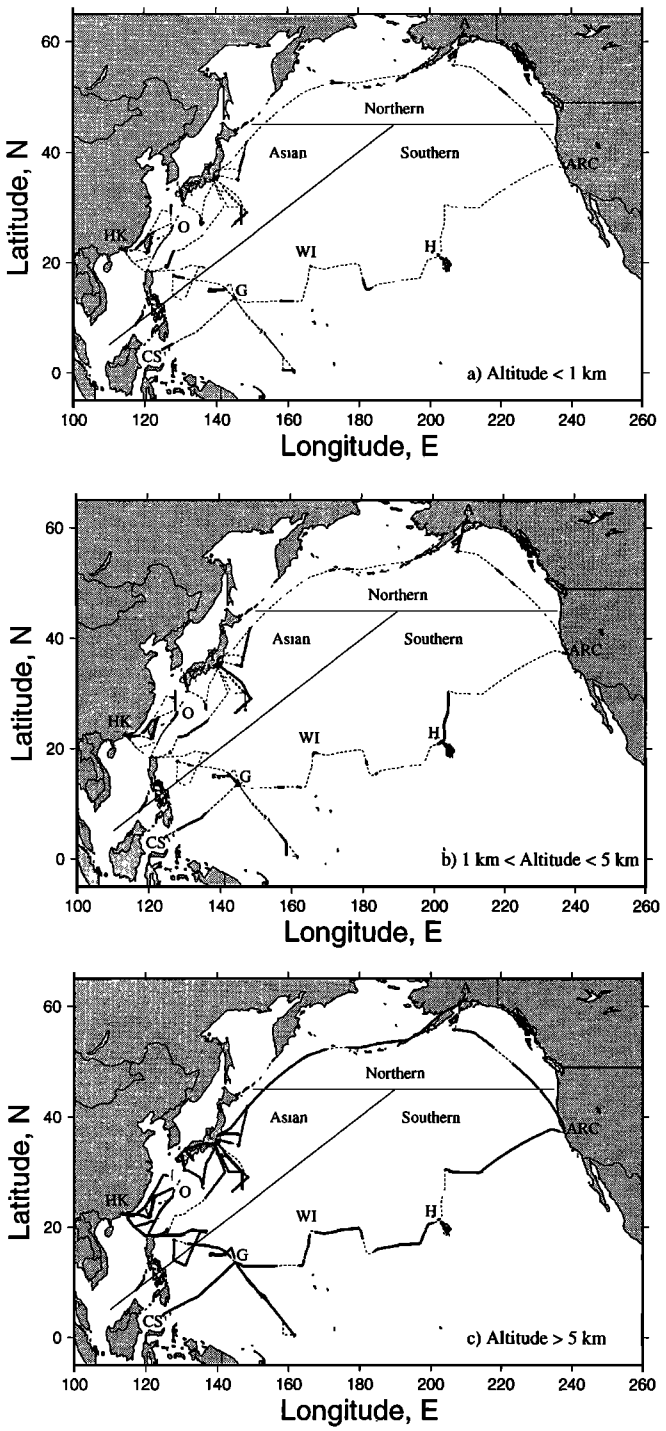

Figure 1. Base map of the PEM-West A study area showing the DC-8 flight tracks, dashed line with thick sections. Thick sections on flight track indicate location of samples for a specific altitude interval: (a) altitude < 1 km, (b) 1 km < altitude < 5 km, and (c) altitude > 5 km. A, Anchorage; ARC, Ames Research Center; CS, Celebes Sea; G, Guam; H, Honolulu; HK, Hong Kong; O, Okinawa; T, Tokyo; and WI, Wake Island. The solid lines split the flights into northern, southern, and Asian subregions.

1961; *Levy*, 1973; *Fishman et al.*, 1979; *Logan et al.*, 1981; *Kleinman*, 1990]. The oxidative state of the atmosphere, determined by whether net ozone production is positive and further by whether there is an excess of peroxyl radicals to produce hydroperoxides, depends critically upon the relative concentration of NO to other constituents, namely, CO, CH_4, and nonmethane hydrocarbons (NMHC) [*Trainer et al.*, 1987; *Lin et al.*, 1988; *Kleinman et al.*, 1990; *Jacob et al.*, 1993]. Observationally, the NO_2 to NO ratio under sunlight conditions has been used to qualitatively evaluate ozone production by how near the ratio is to that predicted assuming steady state among O_3, NO, NO_2, and NO_2 photolysis [e.g., *Stedman and Jackson*, 1975; *Parrish et al.*, 1986; *Carroll et al.*, 1990; *Ridley et al.*, 1992; *Crawford et al.*, this issue; *Davis et al.*, 1993]. A NO_2 to NO ratio higher than prescribed by simple photochemical steady state is suggestive of peroxyl radicals fueling O_3 production. However, before an air mass can be characterized in terms of its net O_3 production, additional information is required concerning O_3 sinks related to water vapor and odd hydrogen radicals [e.g., *Davis et al.*, this issue; *Liu et al.*, 1992]. The hydroperoxide measurements reported here provide insight on the activity of peroxyl radicals, complementing the NO-NO_2-hydrocarbon-based assessment of tropospheric O_3 chemistry in the study region.

The hydroperoxides are directly related to atmospheric odd hydrogen (sum of HO, HO_2, and CH_3OO). HO is the most significant oxidant and cleansing agent of the troposphere [*National Research Council (NRC)*, 1984]. H_2O_2, CH_3OOH, and nitric acid (HNO_3) comprise odd hydrogen reservoirs with their photolysis returning odd hydrogen. The removal of the reservoir compounds through precipitation or dry deposition is one of the principal sinks of odd hydrogen. The other major sink is the reaction of HO with these same reservoir species [*Logan et al.*, 1981]. Measurements of H_2O_2 which are greater than model predictions are suggestive of either higher HO_2 concentrations or slower removal and vice versa [*Liu et al.*, 1992]. However, the sensitivity of modeled H_2O_2 to parameterizations of its removal, at the surface, in-cloud reaction, or by precipitation, obscures its utility near the surface as a constraint on odd hydrogen photochemistry in the lower troposphere [*Heikes*, 1992; *Thompson et al.*, 1993]. However, H_2O_2 in conjunction with CH_3OOH does place bounds on these same parameterizations. The lower solubility of CH_3OOH in water [*Lind and Kok*, 1986, 1994] makes it less dependent on precipitation and surface removal. H_2O_2 rates of production and loss and those for CH_3OOH (lifetimes of the order of days) make them ideally suited to studies of diurnally averaged photochemistry in the middle to upper troposphere but somewhat less applicable to investigations of fast photochemical processes [*Davis et al.*, this issue; J. Rodriguez et al., unpublished material, 1995].

Prior measurements of H_2O_2 and CH_3OOH in the remote Pacific midtroposphere are at variance with photochemical theory. *Liu et al.* [1992] have discussed the contradictions in odd hydrogen radical chemistry posed by the MLOPEX 1988 H_2O_2, CH_3OOH, and CH_2O data of *Heikes* [1992], the nitric acid and nitrate data of *Norton et al.* [1992], and the NO_x to NO_y ratio [*Hubler et al.*, 1992; *Carroll et al.*, 1992]. Most significant was the lower than expected levels of CH_2O and CH_3OOH, both by factors of 2 or greater. H_2O_2 was also smaller than expected but by less than a factor of 2. It will be shown, by the PEM-West A data which follow and by the H_2O_2, CH_3OOH, and CH_2O data of *Heikes et al.* [1993] from MLOPEX 2, that the CH_2O measurements remain at odds with models but that CH_3OOH and H_2O_2 are more in accord with theoretical levels, as was the case for the equatorial Pacific surface layer [*Thompson et al.*, 1993].

The second PEM-West A mission goal concerned the atmospheric sulfur cycle. The conversion of sulfur dioxide (SO_2) and dimethylsulfide to sulfuric acid proceeds through reactions of SO_2 with HO, O_3, H_2O_2, and CH_3OOH in the gas and aqueous phases [e.g., *Penkett et al.*, 1978; *Calvert et al.*, 1985; *Bandy et al.*, 1992; *Kriedenweis and Seinfeld*, 1988]. Measurements of H_2O_2 and CH_3OOH are directly coupled to aqueous sulfur chemistry and indirectly coupled to gas phase sulfur chemistry through their involvement with odd oxygen and odd hydrogen. Hence measurements of peroxides facilitated understanding the sulfur cycle over the western North Pacific.

In the following sections, the hydrogen peroxide and methylhydroperoxide data set is presented. The collection procedures and analytical methods are briefly described. Geographical distributions will be summarized. Hydroperoxides are interpreted with respect to photochemical theory using the results of photostationary steady state and time-dependent point models (Davis et al., this issue; Rodriguez et al., this issue) and a meso-scale 3-D time-dependent photochemical model [*Liu et al.*, this issue; *McKeen et al.*, this issue]. A brief summary discussion of the hydroperoxide concentrations in different air masses is included here and the reader is referred to the following papers in this issue for a presentation of air mass characterization based upon chemistry and meteorology: aged maritime or continental air [*Gregory et al.*, this issue], fresher continental outflow air [*Talbot et al.*, this issue], stratospheric air [*Browell et al.*, this issue], supertyphoon Mireille and typhoon Orchid [*Newell et al.*, this issue (a)], an aged biomass fire plume [*Lee*, 1995], and with respect to a continuous diagnostic measure of air mass processing, the ethyne to carbon monoxide ratio [*Smyth et al.*, this issue].

Experiment

Hydrogen peroxide and methylhydroperoxide were collected in aqueous solution using concurrent flow glass coils and analyzed using two different techniques: the continuous flow procedure of *Lazrus et al.* [1986] modified by *Heikes* [1992] and the high-pressure liquid chromatography (HPLC) method described by *Lee et al.* [1995]. *Heikes* [1992] describes a continuous flow-modulated serial coil method, with the only significant change for PEM-West A being an increase to four channels, which permitted both coils in series to be monitored continuously. In this manner the organic hydroperoxide concentration of the air could be assessed relative to hydrogen peroxide in three ways: using differential catalase enzyme activity, using differential solubility, and using the HPLC system.

The HPLC method was intended to identify and quantify the organic hydroperoxide species collected by the aqueous collection coils of *Lazrus et al.* [1986] and in so doing to verify the common assumption that only methylhydroperoxide be considered in interpreting the catalase enzyme channel in remote atmospheres. Collected samples were to be analyzed post flight for specific hydroperoxides (e.g., H_2O_2, CH_3OOH, or hydroxymethylhydroperoxide). However, hydroxy-methylhydroperoxide and hydroxy-ethylhydroperoxide were found to decompose after an hour or several minutes, respectively, even when stored in an ice-water bath [*Lee et al.*, 1995]. Consequently, the HPLC analyses were performed in flight.

The HPLC system is relatively new and instrumental details may be found in the work of *Lee et al.* [1995]. A $pH = 6$ phthalate buffer solution was used to minimize artifacts due to O_3 and SO_2 during collection [*Lazrus et al.*, 1986; *Lee et al.*, 1995]. Analysis was performed immediately after collection (collection time was typically 5 min). Sample frequency was limited by the difference in elution times for H_2O_2 and CH_3OOH. These were the only hydroperoxides detected by the HPLC system in PEM-West A. Other hydroperoxides would have had to exceed ~100 parts per trillion by volume (pptv) to be quantitatively observed, based upon the detection limits given by *Lee et al.* [1995].

Air samples were brought into the aircraft through a forward facing inlet of 3/8 in. OD (1/4 in. ID) PFA Teflon. An excess of ultra-high-purity (UHP) zero air (liquid carbonics) flowed through the inlet during operation on the ground and at takeoff to minimize contamination of the inlet. The inlet was periodically cleaned with methanol and water. The air sample flow rate for the four-channel system was 3 standard liters per minute (slpm) (STP = 1 atm and 273 K). The aqueous collection solution flow rate was nominally 0.9 mL/min. The HPLC air sample flow rate was 2 slpm and aqueous collection solution flow rate was nominally 0.4 mL/min. Collection solution flow rates were calibrated volumetrically. The air sample flow rates were regulated using low-pressure drop mass flow controllers (MKS Instruments) and remained constant up to a pressure altitude of 10 km; by approximately 12.5 km the flow rates had decreased to 1.8 and 1.3 slpm for the four-channel and HPLC systems, respectively. The decrease in flow was caused by a decrease in pumping efficiency at low pressure.

Collection solution and water blanks were taken by passing UHP zero air through the inlet and collection coil or by diverting the air sample stream through a Hopcolite (Mine Safety Appliance) trap and then into the collection coil. H_2O_2 blanks can be appreciable and variable depending on water quality. A CH_3OOH background in reagent waters has not been observed to date.

Calibrations were performed using at least four different aqueous concentrations of H_2O_2 and CH_3OOH. Standards were prepared by serially diluting primary stock H_2O_2 and CH_3OOH standards. The H_2O_2 stock was prepared by dilution of Ultrex 30% H_2O_2 (J. T. Baker). The primary H_2O_2 stock was standardized by titration using $KMnO_4$ and by UV absorption spectroscopy [*Miller*, 1990]. CH_3OOH was synthesized from dimethylsulfate (Aldrich Chemical Company) and H_2O_2 (J. T. Baker, 30%). The CH_3OOH produced was standardized against the H_2O_2 primary standard using the continuous enzyme fluorescence system and by titration using an iodine-starch procedure [*Lee*, 1995]. The collection efficiency of the coils for H_2O_2 and CH_3OOH was empirically determined by substituting aqueous standards and blanks for the collection solution in the coils. The H_2O_2 collection efficiency was always greater than 98%. The HPLC CH_3OOH collection efficiency ranged from 50 to 65% and the serial coil CH_3OOH collection efficiency was between 60 and 75%. Measured and theoretically derived collection efficiencies for CH_3OOH [see *Lee et al.*, 1995], agreed to within ±10%. A corrected value of the Henry's law constant (1.3 times the value of *Lind and Kok* [1986, 1994]) was used in the theoretical calculation and has since been verified [*O'Sullivan et al.*, 1995]. The uncertainty in the collection efficiency accounts for the largest potion of the estimated uncertainty in the reported concentrations of CH_3OOH. The detection limits for H_2O_2 and CH_3OOH are 30 and 50 pptv, respectively (3 times the standard deviation of the H_2O_2 blank or limit of resolution in the case of CH_3OOH). The estimated accuracy for each at 500 pptv is 70 and 110 pptv, respectively, and at 1000 pptv is 120 and 180 pptv. These were

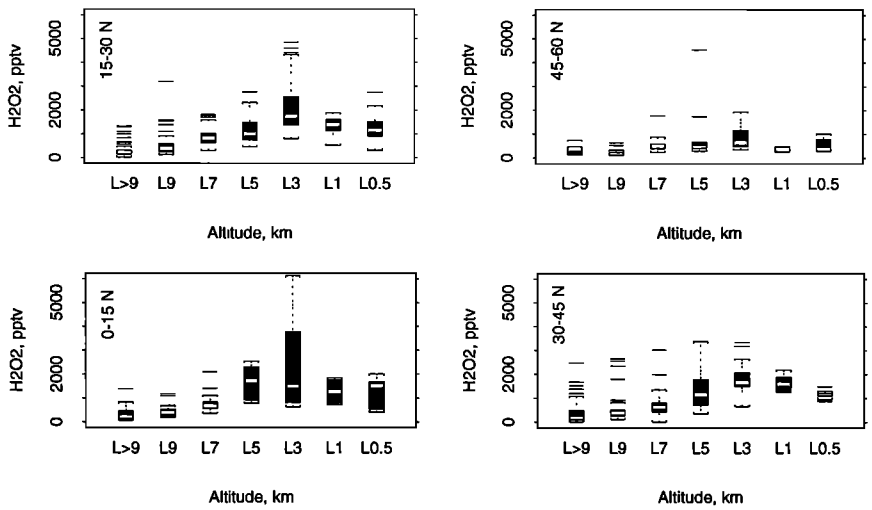

Figure 2. H_2O_2 distributions stratified by latitude (0°–15°N, 15°–30°N, 30°–45°N, and 45°–60°N) and by altitude (0.0–0.5 km (L0.5), 0.5–1 km (L1), 1–3 km (L3), 3–5 km (L5), 5–7 km (L7), 7–9 km (L9), and >9 km (L>9)). Shaded box indicates central 50% of the observations. White central bar indicates median value. Inward facing brackets denote either the limit of observed data or the median ±1.5 times the inner-quartile distance. For normally distributed data, ±1.5 times the inner-quartile distance corresponds to the 95% confidence interval about the mean or median value. Vertical lines beyond the brackets indicate individual observations. Distributions were monomodal.

calculated through a propagation of errors, rounded to the nearest 10 pptv, and included the uncertainties in aqueous peroxide standards, blanks, gas flow rates, aqueous flow rates, and collection efficiency for CH_3OOH.

The suite of instruments flown on board the DC-8 is described by *Hoell et al.* [this issue]. Each instrument had its own duty cycle and time resolution. For the purpose of addressing O_3 and other oxidants and to maximize correspondence to the majority of the other measured species, we have opted to present and discuss our data using the 180-s merged data product from the Georgia Institute of Technology (S. Sandholm, personal communication, 1992). In merging the data from the various groups, four simple guidelines were followed: (1) if a species was not directly measured in the 180-s interval, it was reported as missing (e.g., during a peroxide blank interval); (2) if a species was determined more than once in a 180-s interval, a simple average was used (e.g., O_3, CO); (3) if a species own sample interval spanned more than one 180-s interval, the multiple 180-s values were held constant at the measured value (e.g., nitric acid); and (4) the 180-s averaging period was indexed to the nitric oxide measurements.

Results

The spatial distribution of H_2O_2, CH_3OOH, and the H_2O_2 to CH_3OOH ratio is shown in Figures 2–7. In Figures 2–4 the data were partitioned into four latitude zones: 0°–15°, 15°–30°, 30°–45°, and 45°–60°N. The selection of the zones corresponds to flights into and out of Guam, Hong Kong, Tokyo, and Anchorage. Each zone includes data from at least three or more flights, except for 45°–60°N. There were few measurements at low altitude between 45° and 60°N and care must be

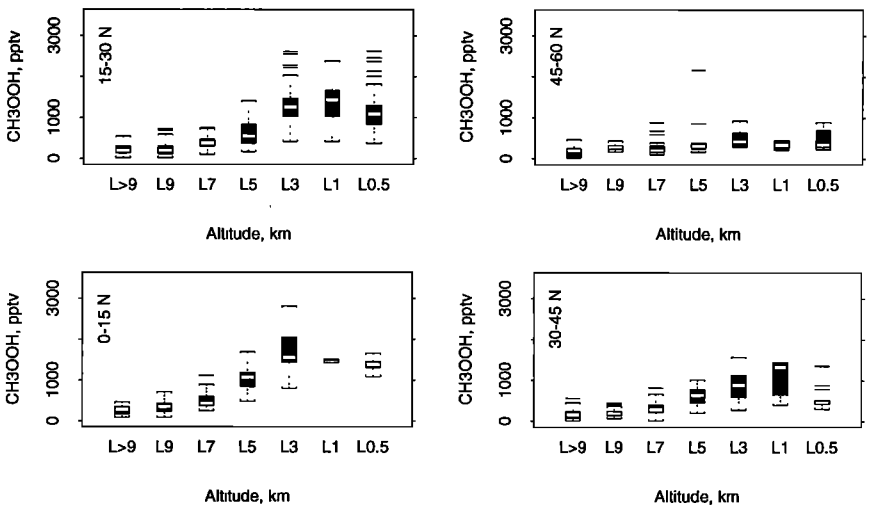

Figure 3. Same as for Figure 2 except for CH_3OOH.

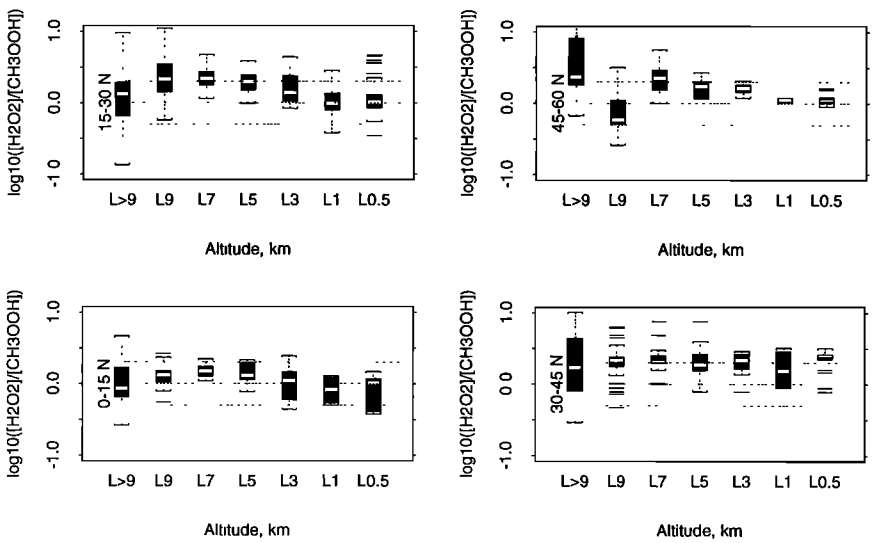

Figure 4. Same as for Figure 2 except for the log base-10 ratio of H_2O_2 to CH_3OOH. Vertical dashed lines indicate ratios of 1:2 or 2:1. Logs are used to provide equal visual weight for a doubling or halving of the ratio.

exercised with regard to the lower-altitude distributions. The data in each latitude belt were further sorted into seven altitude zones: 0–0.5, 0.5–1.0, 1–3, 3–5, 5–7, 7–9, and >9 km, consistent with those used by *Gregory et al.* [this issue]. The population distribution in each latitude-altitude cell is summarized by a box and whisker plot.

H_2O_2 and CH_3OOH both decreased in concentration on moving from the equator toward the pole (Figures 2 and 3). This was evident at all altitudes. There was a prominent maximum in H_2O_2 at altitude, typically 1–3 km, for all latitudes (Figure 2). CH_3OOH maxima also occurred at lower altitudes, typically at 0.5–1 km (Figure 3).

The ratio of H_2O_2 to CH_3OOH is shown in Figure 4. The ratio is plotted as a $\log_{10}$ value to give equal visual weight to ratios less than and greater than 1; for example, ratios of 0.5 and 2 are equally distant from a ratio of 1. There was a tendency for greater amounts of CH_3OOH relative to H_2O_2 in the tropics than at higher latitudes. The latitude trend in the ratio occurred at all altitudes. CH_3OOH decreased relative to H_2O_2 with height. The smallest ratios of H_2O_2 to CH_3OOH were found in the tropical boundary layer and the highest ratios were found at altitude in the 30°–45°N latitude belt. The increased spread in the ratio at altitudes greater than 9 km results, in part, from vertical transport (discussed below) and from both species being nearer their respective detection limits at the highest altitudes.

Geographic distributions of the hydroperoxides are shown in Figures 5–7. The three subregions were chosen to represent the northern transit, near Asia, and Guam and the southern transit (flights 15–21). The subregions are identified in Figure 1. The data were stratified in to three altitude intervals: <1 km, 1–5 km, and >5 km with sample locations indicated by altitude group in Figure 1. The altitude intervals were chosen to highlight the influence of boundary layer processes, the midaltitude maxima, and the high-altitude minima in the peroxide species. H_2O_2 and CH_3OOH during the northern transit (Figure 5) were below 1000 and 500 pptv, respectively, except in the climb out and middle-altitude run off the coast of British Columbia (near 50°N, 218°E). During this flight leg, very high concentrations (4500 and 2000 pptv) of both species were encountered in a thin layer near 5 km. This was most likely a plume from Asia based upon air parcel trajectories. Both species were below their LODs in the lower stratospheric portion of the north transit.

The near-Asia data are presented in Figure 6. CH_3OOH at the upper altitudes is confined to concentrations at or below 500 pptv with occasional spikes near 800 pptv. H_2O_2 on the other hand exhibited a much broader range in concentration (LOD to 3000 pptv). The higher H_2O_2 mixing ratios near 30°N and above 5 km were associated with measurements near and over typhoon Mireille [see *Newell et al.*, this issue (a)], while higher H_2O_2 values between 20° and 25°N above 5 km were associated with deep convective clouds upwind of the aircraft (*Bachmeier et al.* [this issue] flight crew observations). The middle-altitude H_2O_2 and CH_3OOH data show higher levels, in excess of 3000 and 1500 pptv, respectively, in plumes near Asia. Typical H_2O_2 and CH_3OOH values of 1300 and 600 pptv, respectively (north of 20°N), and 1800 and 700 pptv, respectively (south of 20°N), would be expected in air over the ocean which had exited the continent within the last two days [*Talbot et al.*, this issue]. Marine air in the lower troposphere in this region has H_2O_2 and CH_3OOH levels of 1050 and 1500 pptv, with lower levels of H_2O_2 but higher levels of CH_3OOH below 1 km [*Gregory et al.*, this issue].

In general, the southern longitudinal section (Figure 7) showed high CH_3OOH concentrations in the boundary layer, 1000–1500 pptv, from 125°E to Hawaii. At 205°E the concentration dropped to below 1000 pptv. In the lower-tropospheric portion, 1–5 km, CH_3OOH concentrations decreased regularly from 2000 to 500 pptv over this longitudinal range. Above 5 km, CH_3OOH was typically between 250 and 500 pptv. H_2O_2 along this section had higher values in the western Pacific relative to the eastern Pacific at altitudes greater than 5 km. From Guam to Hawaii to Ames, H_2O_2 concentrations remained relatively constant at near 1000 pptv. In the boundary layer, H_2O_2 decreased from near 2000 to 1000 pptv, with a notable exception at 160°E where H_2O_2 was approximately 700 pptv. This occurred on flight 15 at the equator and on flight 18 from Guam to Wake Island at about 13°N. Both sections have H_2O_2 to CH_3OOH ratios near 0.5, suggesting recent removal

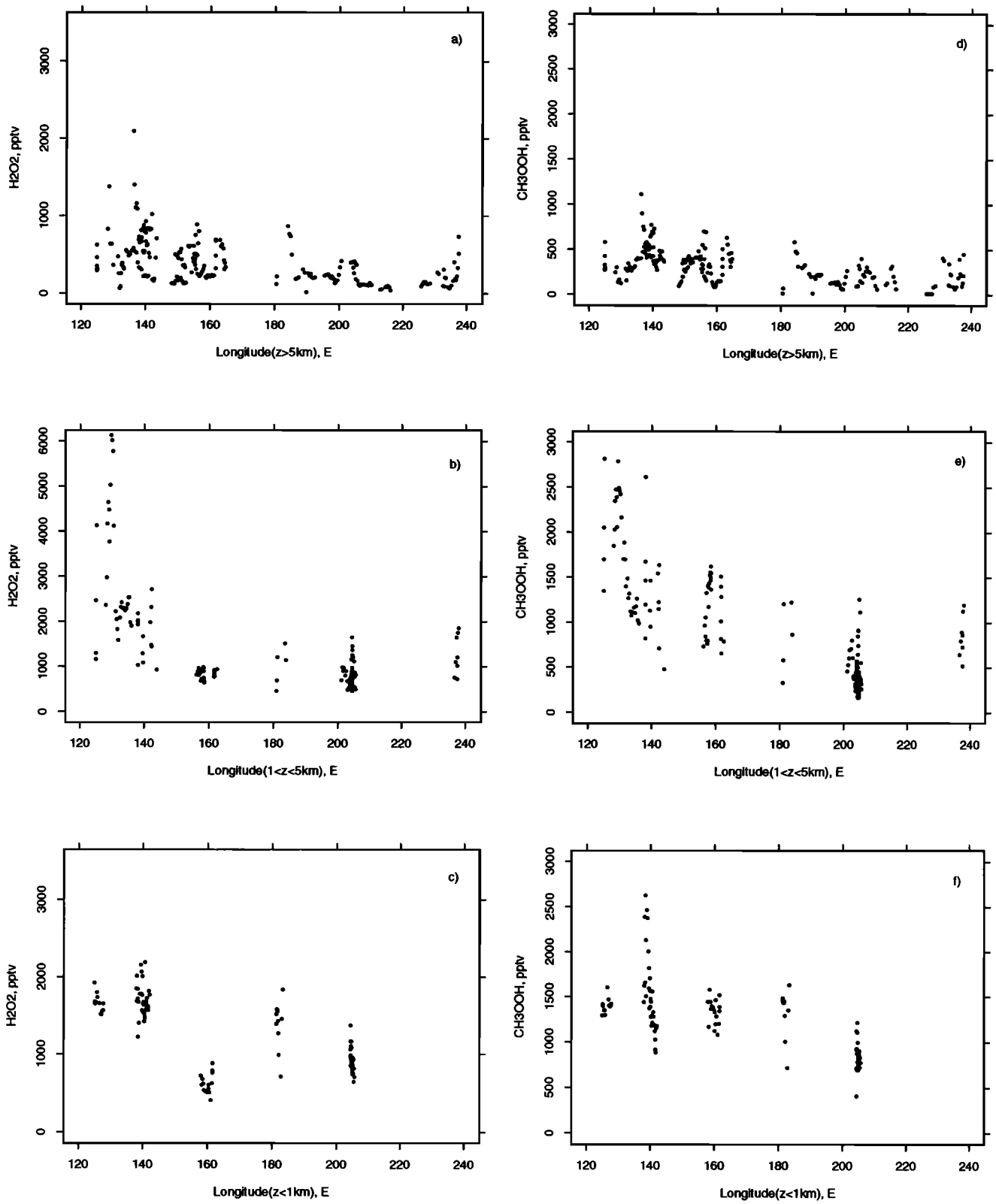

Figure 5. (a–c) H_2O_2 and (d–f) CH_3OOH observations north of 45°N latitude as a function of longitude for three altitude categories: (g and h) <1 km, (e and f) 1–5 km, and (c and d) >5 km. These were primarily transit flight observations. Concentration excursions at a longitude reflect ascent-descent and the strong dependence of concentrations on altitude and compositional layering of the atmosphere. Data correspond to northern subregion identified in Figure 1.

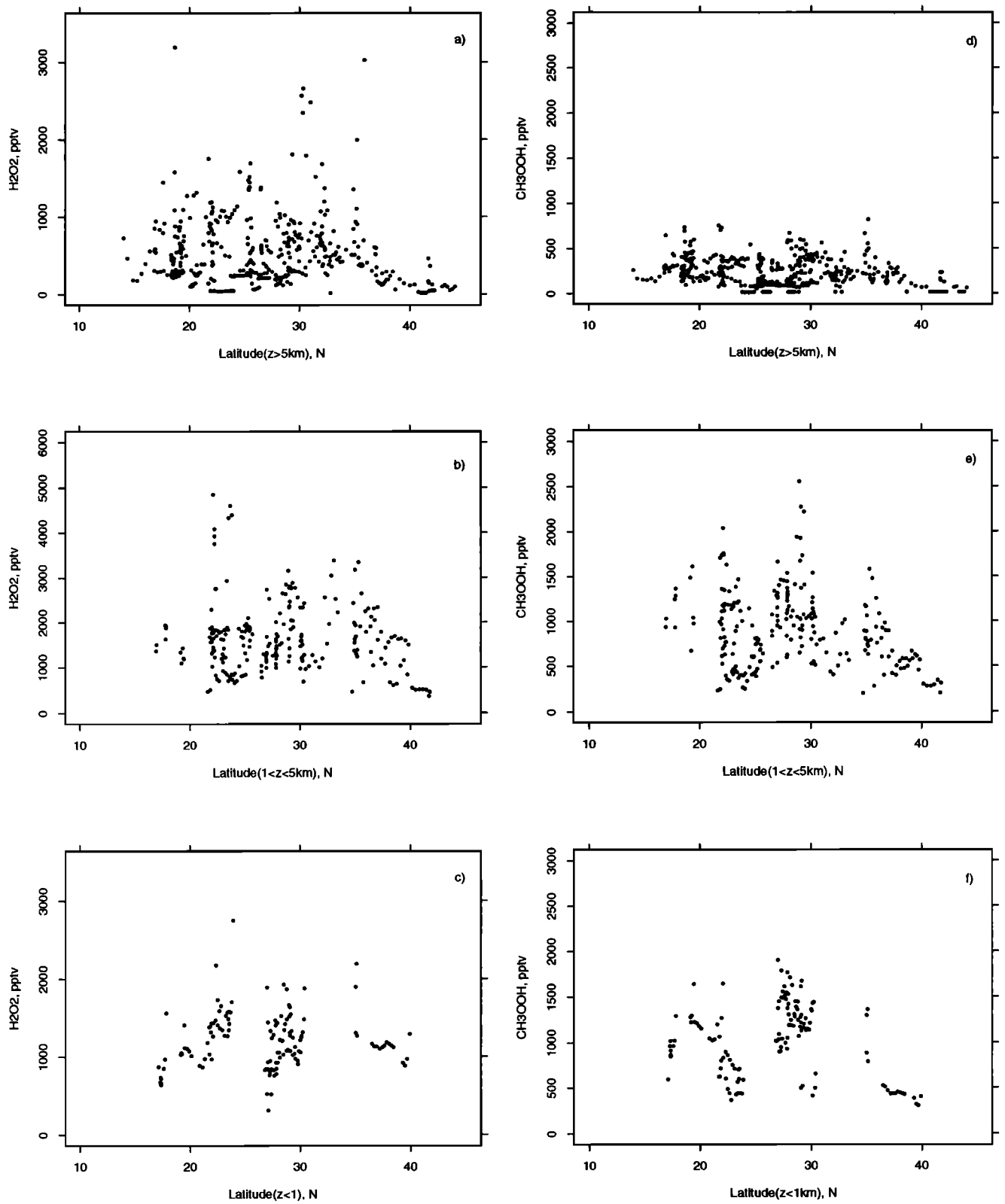

Figure 6. Same as Figure 5 except plotted as a function of latitude and for flights near the Asian continent and include all flights flown out of Japan and Hong Kong and the last part of the transit flight from Alaska to Japan. Data are for Asian subregion indicated in Figure 1.

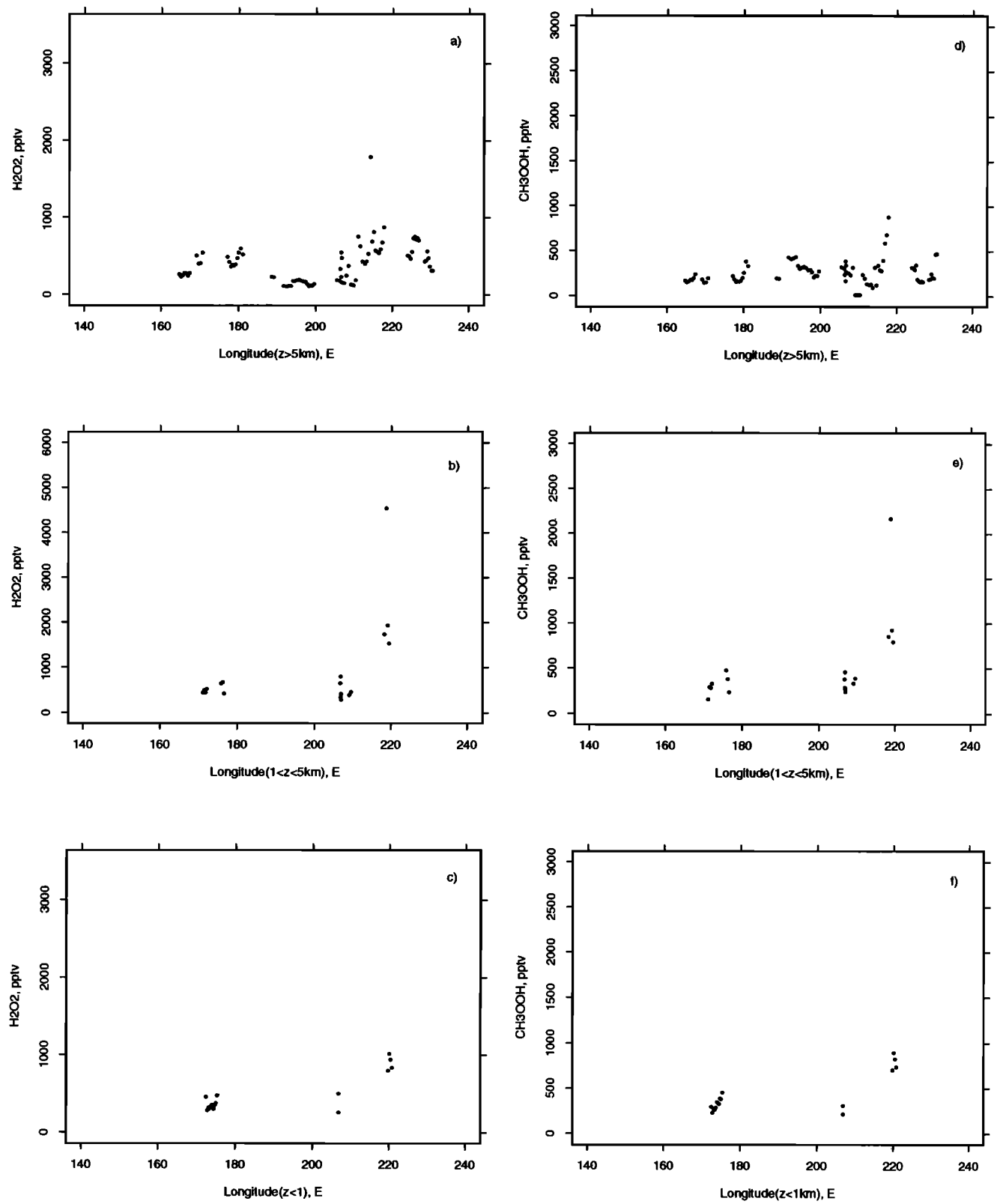

Figure 7. Same as for Figure 5 except for flights farther away from Asia and south of 45°N latitude. These include the Guam, Wake Island, and Hawaii flights and portions of the transit flights from California to Alaska and from Hong Kong to Guam. Observations west of 140°E longitude are impacted by Typhoon Orchid and the Philippines-Indonesia "Island Continent." Data correspond to southern subregion indicated in Figure 1.

of H_2O_2 by precipitation. The highest H_2O_2 (>5000 pptv) and CH_3OOH (>2500 pptv) concentrations for PEM-West A were observed just above the marine boundary layer over the Celebes Sea south of the Philippines (~125°E).

Portions of data were missing from flights 15 to 19 out of Guam because of difficulties with the HPLC system. Gas bubbles formed in the reagents even after they were sparged with helium and allowed to sit for 12 or more hours. The NaOH reagent did not develop bubbles. The gas bubbles were thought to be due to CO_2 outgassing after adding acid to the carbonate-rich waters of Guam, after exposure to high temperatures (T > 30°C) during preflight testing, takeoff, and low-altitude sampling, and from the reduction in cabin pressure during ascent.

Discussion

The PEM-West A H_2O_2, CH_3OOH, and ratio data presented above can be compared with prior measurements over the North Pacific. Data are available from the equatorial boundary layer during SAGA 3 [*Thompson et al.*, 1993; *Heikes and Mosher*, 1990; *Donahue and Prinn*, 1993], the lower free troposphere and modified boundary layer measurements from Mauna Loa Observatory, MLOPEX 1988 and MLOPEX 2 [*Heikes*, 1992; *Heikes et al.*, 1993], the EMEX flights [*Lind et al.*, 1987], and PSI measurements off the coast of Washington [*Lee and Busness*, 1989]. In general, the measurements reported here are consistent with those for H_2O_2 and CH_3OOH. However, it appears that the MLOPEX 1988 measurements of CH_3OOH were either anomalously low or in error (B. G. Heikes, personal communication, 1993). Our data near Hawaii, the data of *Lind et al.* [1987] near Hawaii, and the recent data of *Heikes et al.* [1993] at Mauna Loa Observatory, showed much higher concentrations of CH_3OOH at or near Hawaii and throughout the Pacific than were measured during May and early June 1988. Also, the ratio of H_2O_2 to CH_3OOH reported here is between 1 and 2, whereas during MLOPEX 1988 it was closer to 8. A ratio of 1–2 would be more in keeping with photochemical models of the remote atmosphere [*Logan et al.*, 1981; *Liu et al.*, 1992]. The concentrations of H_2O_2 observed below 500 m in the equatorial Pacific were similar to those observed during SAGA 3 at 6.5 m. Our CH_3OOH concentrations are about twice those observed and modeled in SAGA 3 and the ratio of H_2O_2 to CH_3OOH is approximately ½ that observed in SAGA 3 [*Thompson et al.*, 1993].

Talbot et al. [this issue] and *Gregory et al.* [this issue] have characterized marine air and continental air masses based upon the meteorological back trajectories of *Merrill* [this issue]. *Smyth et al.* [this issue] have presented an air mass characterization scheme based upon hydrocarbon ratios and *Browell et al.* [this issue] have characterized the atmosphere based upon aerosol backscatter, ozone, and potential vorticity [*Newell et al.*, this issue (b)]. H_2O_2 was at or below our detection limit and CH_3OOH was always below our detection limit in air that was classified as stratospheric air [*Browell et al.*, this issue].

North of 20°N, H_2O_2 was 370 pptv greater in continental outflow than in marine air, from the data presented by *Gregory et al.* [this issue] and *Talbot et al.* [this issue] for altitudes above the boundary layer. South of 20°N, H_2O_2 was 310 pptv higher in continental outflow than in aged marine air. The differences noted between continental and marine air for CH_3OOH were smaller than those for H_2O_2 and were +90 and −70 pptv for the cases north and south of 20°N, respectively. The H_2O_2/CH_3OOH ratio was about 2.25 in continental outflow and is 1.8 in north marine air and 0.9 in south marine air. *Smyth et al.* [this issue] presented the ethyne to carbon monoxide ratio, C_2H_2/CO, as a measure of air mass processing, be it through photochemical oxidation (principally HO) or the mixing of fresher air (continentally influenced air masses) with well-processed air. The higher the ratio the more recent an air mass was exposed to surface emissions. Their processing factor is fundamentally similar to the C_3H_8/C_2H_6 ratio used by *Kondo et al.* [this issue]. Observed H_2O_2 was independent of the C_2H_2/CO ratio or processing factor. On the other hand, CH_3OOH increased with atmospheric processing or decreased C_2H_2/CO ratio. Consequently, the H_2O_2/CH_3OOH ratio also decreased with processing, consistent with the evaluated trends in continental and marine air masses noted in the data of Talbot et al. and Gregory et al. The trend in CH_3OOH was thought to be related to HO competition between CH_4 and other hydrocarbons and a concomitant increase in methylperoxyl in processed air.

The most notable feature of the southern section was the hydroperoxide concentrations observed over the Celebes Sea south of the Philippines (Figure 7). A layer of enhanced aerosols and other chemical components was observed and sampled just above the marine boundary layer. Hydrocarbon, halocarbon, oxides of nitrogen, carbon monoxide, and other data suggested this region contained aged biomass burning and urban emissions [*Blake et al.*, this issue]. The hydroperoxide concentrations in this layer were the highest encountered during the PEM-West A project, 6000 and 3000 pptv for H_2O_2 and CH_3OOH, exceeding those encountered on takeoff at Yokota (2000 and 1000 pptv) and at Hong Kong (4500 and 1500 pptv) (see Figure 6). Fires were thought to be associated with the highest hydroperoxide and formaldehyde concentrations in MLOPEX 1 [*Heikes*, 1992]. In the TRACE A experiment, over southern Africa and Brazil in fall 1992, extremely high hydroperoxide concentrations and formaldehyde concentrations were observed in air near active biomass fires (M. Lee et al., manuscript in preparation, 1995). The impact of biomass fire emissions on hydroperoxides are discussed in detail by *Lee* [1995] and M. Lee et al. (1995).

The occurrence of a maxima in the hydroperoxides at altitude, Figures 2 and 3, usually manifested itself as a sharp break in concentration just above the surface mixed layer and has been documented by others [e.g., *Heikes et al.*, 1987; *Lee and Busness*, 1989; *Van Valin et al.*, 1991]. It is interesting to note the two species peak at slightly different altitudes, CH_3OOH below H_2O_2. This was considered to be the result of H_2O_2 surface deposition being greater than that for CH_3OOH. Both the point model [*Crawford et al.*, this issue; *Davis et al.*, this issue] and the three-dimensional model [*Liu et al.*, this issue; *McKeen et al.*, this issue] reproduced the hydroperoxide trends with latitude and altitude. However, both overestimated median H_2O_2, by more than its inner-quartile distance, at the lower altitudes (<3 km). The H_2O_2 overprediction could have been the result of underestimating surface dry deposition or precipitation scavenging; no surface removal process was included in the point model. The three-dimensional model also overestimated H_2O_2 at the higher altitudes, where assumed lateral boundary concentrations were more important than local photochemistry in establishing H_2O_2 concentrations within the model domain [see *Liu et al.*, this issue].

In addition to the geographical comparison of modeled and measured concentrations of hydroperoxides, the PEM-West A measurements included several species whose concentrations

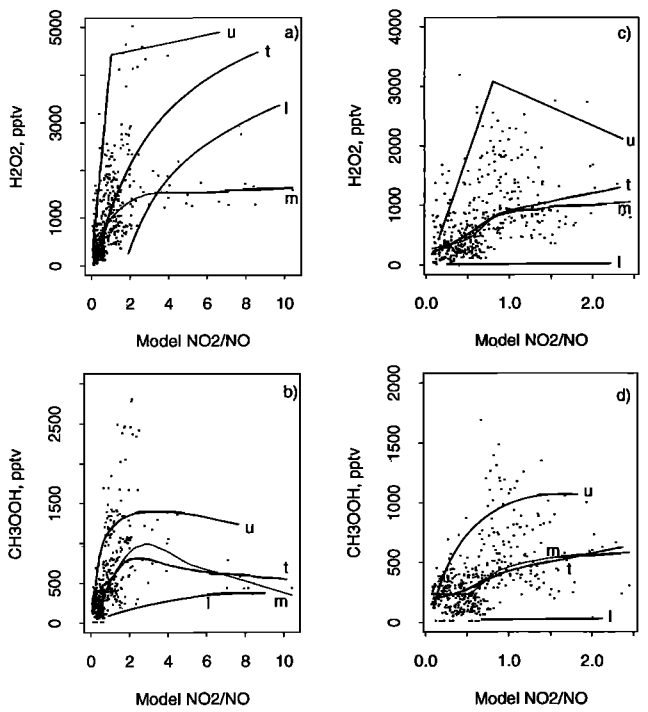

Figure 8. H_2O_2 and CH_3OOH as a function of the NO_2 to NO ratio. Observations are used only when solar elevation angles are greater than 30°. NO concentrations are greater than 3 times their standard deviation. NO_2 was taken from the model of *Crawford et al.* [this issue] for reason given therein. All observations are shown. Measurement trend lines, labeled "m," were computed using local weighted smoothed scatterplot routine, LOWESS (Splus, Statistical Sciences, Incorporated, Seattle). (a and b) All data available meeting the above criteria and (c and d) a fourth constraint of altitudes greater than 3 km. Curves labeled u, l, and t indicate point model upper limit, lower limit, and trend line, respectively.

and, more importantly, interspecies ratios can be used to examine the chemical functionality of the models as they are related to hydroperoxide concentrations. The evaluation of complex photochemical models with direct field measurements is often confounded by model initial and boundary conditions and by the limited spatial and temporal extent of the data, but the characteristics of the model (e.g., O_3, H_2O_2, or CH_3OOH as a function of NO_x and hydrocarbons or products of each other) can be explored by such data [e.g., *National Center for Atmospheric Research* (*NCAR*) 1986]. The ratio of NO_2 to NO, while clearly dependent upon O_3, actinic flux and temperature, should also be dependent upon peroxyl radical concentrations on timescales of a few minutes to tens of minutes. H_2O_2 and CH_3OOH concentrations are also related to peroxyl radicals and through them to the NO_2/NO ratio. Figure 8 shows the relationship between H_2O_2 or CH_3OOH and the NO_2 to NO ratio for all altitudes and for altitudes greater than 3 km. The measurement trend line, labeled m, is computed using a local weighted smoothed scatterplot routine, LOWESS (Splus, Statistical Sciences Incorporated, Seattle). NO_2 data are taken from the model of *Crawford et al.* [this issue] for reasons given therein. A subset of the entire data set was selected using these criteria: NO > 3 times the standard deviation of its signal and solar elevation angle >30°. Two plots are given for all data meeting these criteria and for those data from altitudes greater than 3 km. From an examination of Figure 2 it was believed H_2O_2 data from above this height would be relatively free of the effects of surface removal and more clearly reflect photolytic sources and sinks. The range and trend line for the steady state point model predictions are given by the lines labeled u, l, and t, respectively. Direct model-measurement point comparisons are presented by *Davis et al.* [this issue] and shown below. The model does a good job of capturing the data ranges and trends above 3 km for both H_2O_2 and CH_3OOH and for CH_3OOH at all altitudes. It overpredicts H_2O_2 at NO_2/NO ratios >4 in the lower altitudes and this was considered to be the result of surface deposition. The underprediction of CH_3OOH was most likely due to an underestimate of CH_3OO, since H_2O_2 and HO_2 appeared to be well represented.

In the remote free troposphere the production and cycling of odd hydrogen between HO, HO_2 and CH_3OO are dependent upon the spectral intensity of light, temperature, O_3, H_2O, CO, CH_4, and the reactive oxides of nitrogen (NO_y). The production rate of HO is proportional to O_3-to-O^1D photolysis rate, O_3, and H_2O, and its loss is proportional to CO and CH_4. For the purpose of discussing HO, CH_4 in PEM-West A was effectively constant and $[HO]^{-1}$ will be proportional to the ratio $[O_3{*}H_2O/CO]^{-1}$. The reaction of HO with CO yields HO_2 and the reaction of HO with CH_4 yields CH_3OO. The peroxyl radicals can react with NO or react with each other to produce hydroperoxides. The former gives rise to NO_2 and increased odd oxygen. Some odd hydrogen will be sequestered in HNO_3 and some in hydroperoxides. Both the data and the models were expected to yield positive correlations between H_2O_2 or CH_3OOH and the $O_3{*}H_2O/CO$ or $O_3{*}H_2O/NO_y$ ratios. These relationships are shown in Figures 9 and 10 for the observed data and for the modeled data of *Davis et al.* [this issue] and *Crawford et al.* [this issue], DC, and the model data of *Liu et al.* [this issue] and *McKeen et al.* [this issue], LM. The solid line shows the LOWESS curve through the observations. The LOWESS approach is appropriate for data exploration when the functionality between variables is unknown. The dashed line is that for the DC model and the dotted line is that for the LM model. The LM data come from simulations and grid cells selected at times and locations bounding those of actual flights. The DC data come from photochemical steady state point model simulations of actual in-flight data in which H_2O_2, CH_3OOH, HNO_3, and NO_2 were predicted. Only data from above 3 km are shown. The measurements and data exhibited a monotonic increase in hydroperoxides with increasing $O_3{*}H_2O/CO$. Both hydroperoxides increased with increasing radical production and less NO_y. There was a more dramatic change in slope with increasing $O_3{*}H_2O/NO_y$ ratio than shown for increasing $O_3{*}H_2O/CO$. The models simulated the functional trends found in the measurements. However, at a specific ratio the LM model indicated more H_2O_2 (~2 times) and CH_3OOH (~500 pptv) than measured or predicted by the DC point model. The merits and deficiencies of the LM model with respect to all measurements are discussed in detail by *Liu et al.* [this issue] and *McKeen et al.* [this issue].

Photostationary state point models [e.g., *Davis et al.*, this issue; J. Rodriguez et al., unpublished material, 1995] were used to evaluate the net production rate of odd oxygen and odd hydrogen or the oxidative capacity of the atmosphere. These models provided direct estimates of the free radical concentrations of HO, HO_2, and CH_3OO at the location of the aircraft and will be used here to further examine the relationship between the hydroperoxides and odd oxygen and odd hydro-

gen. The two point models gave virtually identical results and only the DC model results are used here. Calculated odd hydrogen concentrations are presented for a subset of the measurement conditions: NO > 3 sigma, altitude (z) > 3 km, solar elevation angle > 30°, H_2O_2 > 30 pptv, and CH_3OOH > 50 pptv. These conditions ensure confidence in the application of the unconstrained version of the photochemical stationary state point model. Predicted values of H_2O_2 and CH_3OOH are plotted against their respective measured values in Figure 11. The modeled CH_3OOH showed a better linear fit to the measurements (r^2 = 0.72) than did H_2O_2 (r^2 = 0.58) with, however, a tendency to more greatly underpredict its concentration, slope = 0.72. The H_2O_2 slope was 0.85. Slopes were calculated using the line of organic correlation method [*Hirsch and Gilroy*, 1984]. NO_2 was also underestimated by the model and this is discussed more fully by *Crawford et al.* [this issue]. The low values for these three species are suggestive of model HO_2 and CH_3OO being too low. However, the following caveats are in order: (1) NO_2 photolysis rates could be too high [*Davis et al.*, this issue] resulting in greater NO turnover and reductions in peroxyl concentrations; (2) extreme differences in H_2O_2 and CH_3OOH may result from advection or mixing, since photochemical steady state may not be maintained during rapid transport and heterogeneous cloud processes were not considered in the model; (3) measured NO_2 concentrations could be too high due to artifacts or interferences [*Crawford et al.*, this issue].

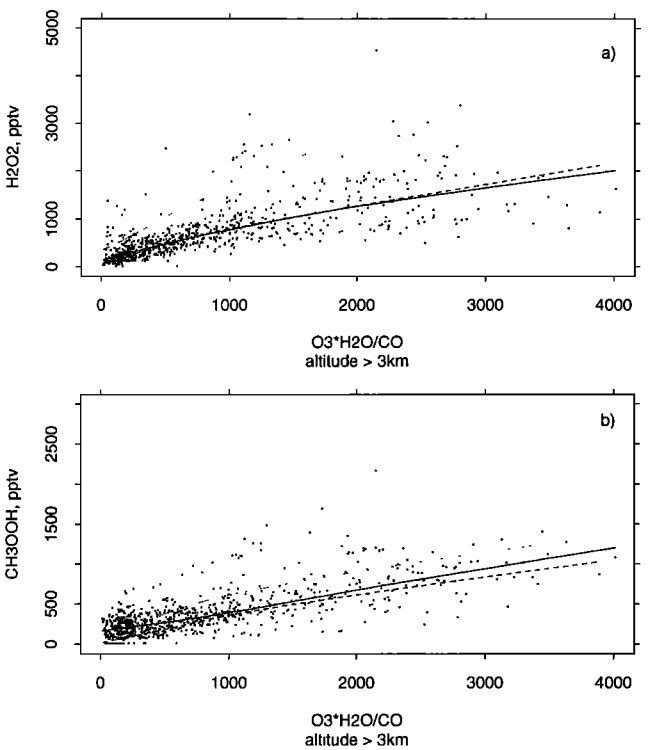

Figure 9. H_2O_2 and CH_3OOH as a function of the O_3 times H_2O to CO ratio for observations at altitudes greater than 3 km. The solid line is the LOWESS curve for the observations (individual points). The dashed line is the LOWESS curve for the unconstrained photochemical model predictions of *Crawford et al.* [this issue] and *Davis et al.* [this issue]. The dotted line is the LOWESS curve through the three-dimensional model predictions of *Liu et al.* [this issue] and *McKeen et al.* [this issue]. Three-dimensional model data were limited to grid cells near the flight tracks.

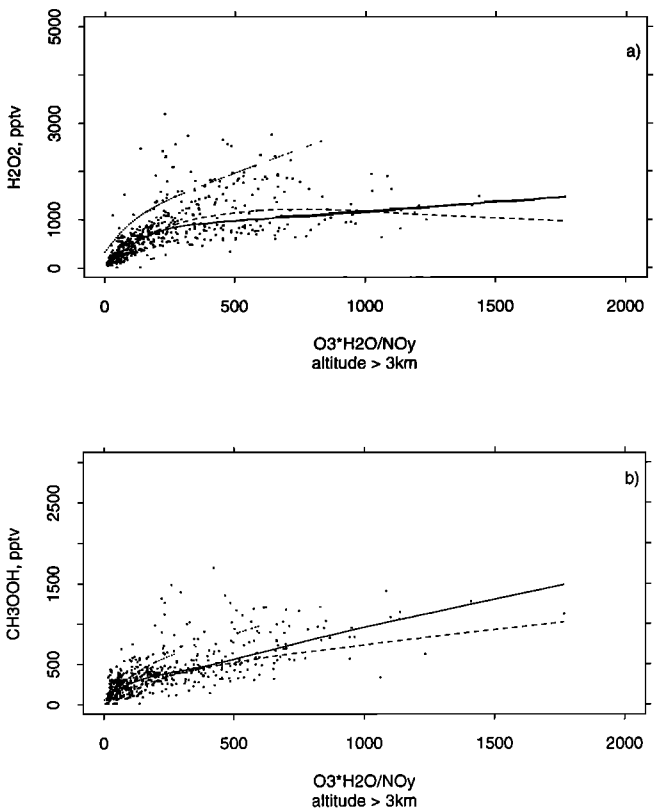

Figure 10. Same as for Figure 9 except as a function of the O_3 times H_2O to NO_y ratio.

The impact of surface deposition on point-model-calculated H_2O_2 and CH_3OOH was explored. Time-dependent calculations were performed for chemical conditions typical of boundary layer marine air north of 20°N and south of 20°N latitude. Surface removal for H_2O_2 and CH_3OOH was represented by a first-order loss rate. Model and measured H_2O_2 concentrations could be made equal by using a surface loss e-fold time of about 3.5 days. CH_3OOH modeled and measured values could not be resolved by adjusting its surface removal rate, with measured values being approximately 20% higher than model predictions. One scenario to bring both species into better agreement would involve increasing model CH_3OO, HO_2, and HO while increasing the surface deposition of H_2O_2 relative to CH_3OOH. Higher peroxyl radical concentrations would also bring the higher-altitude measurements and modeled values into better agreement. *Heikes et al.* [1995] have argued for H_2O_2 and CH_3OOH deposition velocities of 0.8 and 0.6 cm/s over the South Atlantic which yielded surface deposition loss time constants of the order of 1–2 days, more rapid rates of loss for both species than indicated above for H_2O_2 alone.

The ratio of HO to HO_2 and the ratio of HO to CH_3OO should be proportional to the ratio of NO to CO to a first approximation in a remote atmosphere. The resultant steady state ratio of H_2O_2 to CH_3OOH may also depend upon the NO to CO ratio. These trends are examined in Figure 12, where a linear relationship is seen between the above species ratios and the ratio of NO to CO for steady state model conditions. Figure 12d shows the measured ratio of H_2O_2 to CH_3OOH versus the measured NO to CO ratio and Figure 12e

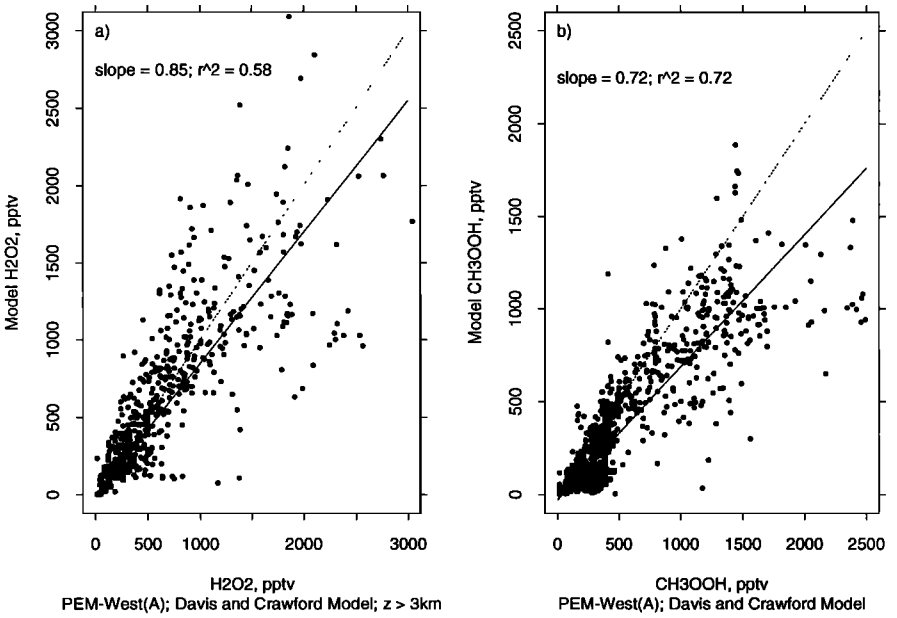

Figure 11. Comparison of photochemical steady state (a) H_2O_2 and (b) CH_3OOH with measured concentrations. Observations from above 3 km were selected to avoid the influence of surface removal on H_2O_2. The dashed line indicates 1:1 correspondence. The solid line indicates the line of organic correlation [*Hirsch and Gilroy*, 1984] with the slope and coefficient of determination given in each panel.

shows the peroxide ratio plotted against the modeled HO_2/HO ratio. There is considerably more scatter in the measured H_2O_2/CH_3OOH ratios than in the modeled ratios, Figures 12c and 12e. Most striking was the measured ratios less than 1 ($\log_{10}$ [ratio] = 0) with values approaching 0.1. None of the modeled ratios are below 1. One possible explanation for this involved vertical transport with H_2O_2 removal by precipitation or in-cloud chemistry.

The measurements of H_2O_2, CH_3OOH, and their ratio provided insight on the recent processing of sampled air masses by cloud and precipitation. There are three possible fates for H_2O_2 when transported through cloud; removal by precipitation, reaction with SO_2 in cloud particles, or transport through the cloud unaltered. The occurrence of high H_2O_2 above 5 km (Figure 6c) and its increase relative to CH_3OOH (Figure 6d) appeared to be associated with convective activity. *Dibb et al.* [this issue] showed similar features in the near-Asia ^{210}Pb, ^{7}Be, aerosol, and acidic gases data. The enhancement in H_2O_2 was contrary to expectations based upon measurements in high SO_2 environments (eastern North America), in which aqueous reactions between H_2O_2 and SO_2 and precipitation removal would reduce peroxide levels during convection in cloud (B. G. Heikes, unpublished data, 1988). However, these findings were in agreement with a recent numerical cloud experiment using SO_2 levels consistent with those reported for PEM-West A by *Thornton et al.* [this issue]. The *Wang and Chang* [1993a, b] model predicts reduced H_2O_2 concentrations in the immediate vicinity of a convective cloud and enhanced H_2O_2 downwind of the cloud as a result of transport effects, aqueous reactions, and gas phase photochemical reactions.

In subtle contrast, it can be seen from Figure 4 that above 3 km, hydroperoxide ratios less than 0.7 were found only at the higher altitudes, above 7 km. Transport alone should enhance both H_2O_2 and CH_3OOH with their ratio expected to remain equal to the low-altitude value or to increase upon mixing with middle and upper level air containing relatively more H_2O_2 than CH_3OOH. The SO_2 data [*Thornton et al.*, this issue] aided in interpreting the H_2O_2 data. If SO_2 is present in air passing through cloud, it will react with H_2O_2 and reduce its concentration relative to CH_3OOH. In the cases, in which H_2O_2 was depleted (<200 pptv) relative to CH_3OOH (>250 pptv), SO_2 concentrations were in excess of 100 pptv and at times near 300 pptv, concentrations which were near or in excess of the observed H_2O_2 concentration. In the earlier convective cases when H_2O_2 was elevated, CH_3OOH was also elevated and SO_2 was below 100 pptv and often below 50 pptv. This indicated H_2O_2 was well in excess of SO_2 and a significant fraction of the H_2O_2 could have passed through cloud without depletion.

Additional indications on convective transport was gleaned from the oxides of nitrogen data. HNO_3 is soluble and will be removed from air which has experienced precipitation. Limited HNO_3 data were available at the times of the H_2O_2 cases of interest and it was necessary to invoke a surrogate measure of HNO_3 in order to examine these cases. The surrogate was calculated by subtracting the observed concentrations of NO_2, NO, and PAN from NO_y. When H_2O_2 was high, the HNO_3 surrogate was between 300 and 500 pptv. Conversely, when H_2O_2 appeared to be depleted with respect to CH_3OOH, the HNO_3 surrogate was between 200 and 300 pptv. For the few cases with measured HNO_3, HNO_3 was 40 pptv when the H_2O_2/CH_3OOH ratio was less than 1 and it was 40–300 pptv when H_2O_2 was high. Formic acid showed a trend similar to HNO_3 or its surrogate, but acetic acid concentrations were the same in both sets of cases.

The behavior of the soluble species and their less soluble cohorts suggested their future use as indicators of recent vertical motion with and without reaction and with and without precipitation. Deviation from photochemical steady state will be a transient phenomenon, and in the cases of H_2O_2 and CH_3OOH they should return to steady state values within a

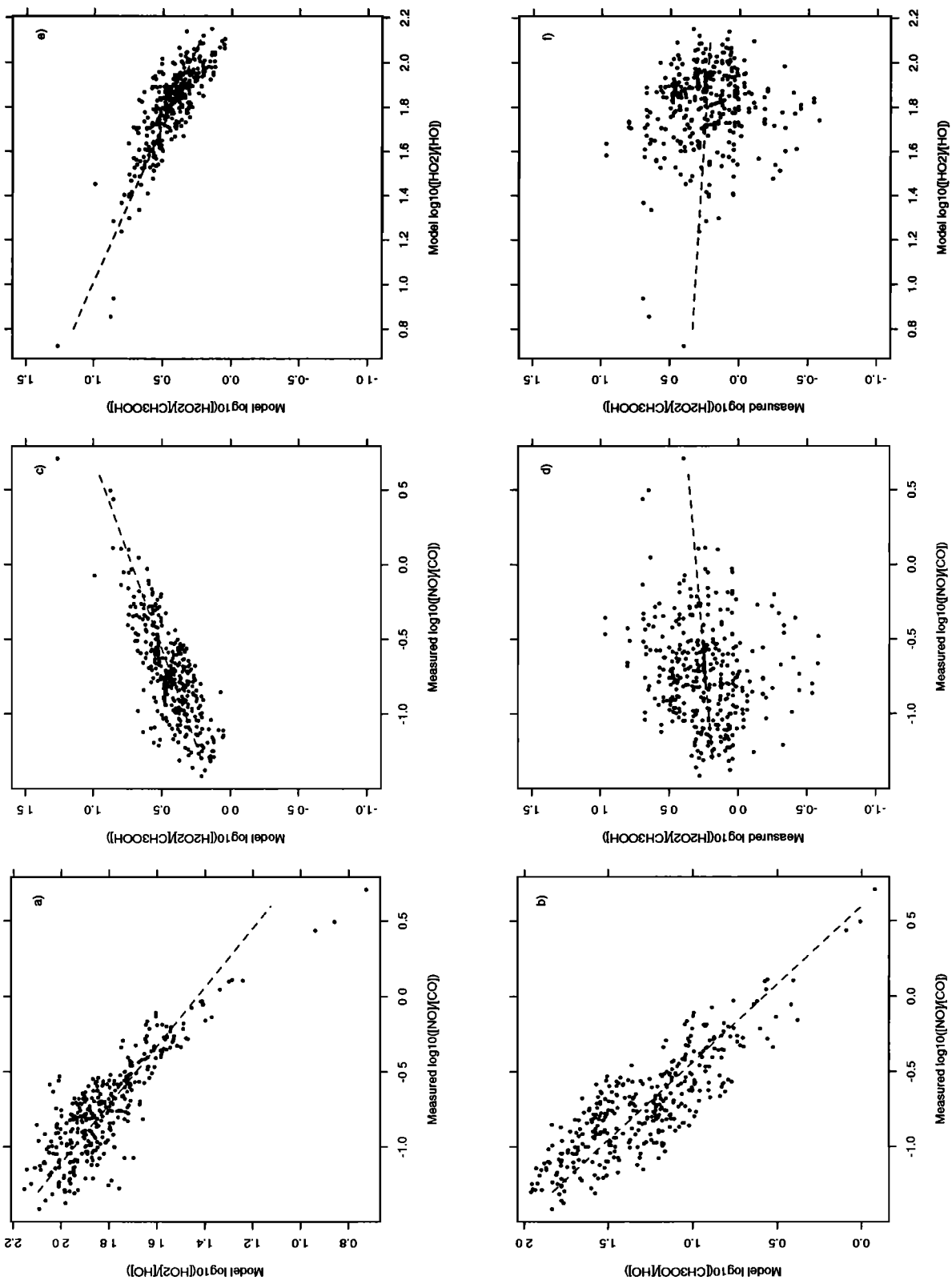

Figure 12. Relationships between photochemical steady state HO, HO_2, CH_3O_2, H_2O_2, and CH_3OOH concentration ratios as a function of observed NO/CO ratio and measured H_2O_2 and CH_3OOH ratios as a function of predicted HO_2/HO ratio and measured NO/CO ratio. Note that ratios were calculated with NO in units of parts per trillion by volume and CO in units of parts per billion by volume; actual NO to CO ratios would be 1000 times smaller.

couple of days as their photochemical lifetimes were both of the order of a day during PEM-West A. Hence their diagnostic utility will be temporally restricted to times less than this.

Conclusions

H_2O_2 and CH_3OOH distributions have been presented for the North Pacific in the fall of 1991. Both species decreased with latitude. H_2O_2 exhibited a strong lower to middle altitude maximum, with concentrations decreasing with lower altitudes due to surface removal and decreasing with increasing altitude due to a decrease in radical precursors and H_2O. CH_3OOH also showed a lower- to middle-altitude maximum with a slight decrease with decreasing altitude due to surface deposition or a reduction in source strength (HO titrated by hydrocarbons and nitrogen dioxide and with less HO produced due to lower ozone), and the decrease with increasing altitude being steeper relative to H_2O_2. CH_3OOH concentrations were directly coupled to HO, whereas H_2O_2 is more strongly coupled to HO loss and the consequent formation of HO_2.

Photochemical models (steady state point, time-dependent point, and three-dimensional time dependent), represented well the values, trends, and photochemical relationships between the hydroperoxides and other measured parameters, notably the oxides of nitrogen, nonmethane hydrocarbons, ozone, water, methane, and carbon monoxide. Exceptions were noted in the boundary layer where surface removal of H_2O_2 is important and in the upper altitude regions thought to be impacted by recent vertical transport. These regions where characterized by either enriched or depleted concentrations of H_2O_2 relative to CH_3OOH depending upon whether SO_2 was present at high levels or precipitation was inferred.

Acknowledgments. This research was supported by the National Aeronautics and Space Administration Global Tropospheric Experiment. SL and SM were supported in part by the Atmospheric Chemistry Project of the Climate and Global Change Program of the National Oceanic and Atmospheric Administration and by the NASA Global Tropospheric Experiment. BGH and ML thank G. Kok for sharing his efforts on the HPLC methodology for hydroperoxides. The Electric Power Research Institute is acknowledged for their support of our development of the hydrogen peroxide and methylhydroperoxide methodology.

References

Bachmeier, A. S., R. E. Newell, M. C. Shipham, Y. Zhu, D. R. Blake, and E. V. Browell, PEM West A: Meteorological overview, *J. Geophys. Res.*, this issue.

Bandy, A. R., D. L. Scott, B. W. Bloomquist, S. M. Chen, and D. C. Thorton, Low yields of SO_2 from dimethyl sulfide oxidation in the marine boundary layer, *Geophys. Res. Lett.*, *19*, 1125–1127, 1992.

Blake, D., et al., Three-dimensional distributions of NMHC and halocarbons over the North Pacific during the 1991 PEM-West A, *J. Geophys. Res.*, this issue.

Browell, E. V., et al., Influence of stratospheric intrusions on the chemical composition of the troposphere over the western Pacific During PEM-West A, *J. Geophys. Res.*, this issue.

Calvert, J. G., A. Lazrus, G. L. Kok, B. G. Heikes, J. G. Walega, J. Lind, and C. A. Cantrell, Chemical mechanisms of acid generation in the troposphere, *Nature*, *317*, 27–35, 1985.

Carroll, M. A., et al., Aircraft measurements of NO_x over the eastern Pacific and central United States and implications for ozone production, *J. Geophys. Res.*, *95*, 10,205–10,233, 1990.

Carroll, M. A., B. A. Ridley, D. D. Montzka, G. Hubler, J. G. Walega, R. B. Norton, B. J. Huebert, and F. Grahek, Measurements of nitric oxide and nitrogen dioxide during the Mauna Loa Observatory photochemistry experiment, *J. Geophys. Res.*, *97*, 10,361–10,374, 1992.

Crawford, J., et al., Photostationary state analysis of the NO_2-NO system based on airborne observations from the western and central North Pacific, *J. Geophys. Res.*, this issue.

Davis, D. D., et al., A photostationary state analysis of the NO_2-NO system based on airborne observations from the subtropical/tropical North and South Atlantic, *J. Geophys. Res.*, *98*, 23,501–23,523, 1993.

Davis, D. D., et al., Assessment of ozone photochemistry in the western North Pacific as inferred from PEM-West A observations during fall 1991, *J. Geophys. Res.*, this issue.

Dibb, J. E., R. W. Talbot, K. I. Klemm, G. L. Gregory, H. B. Singh, J. D. Bradshaw, and S. T. Sandholm, Asian influence over the western North Pacific during the fall season: Inferences from lead 210, soluble ionic species and ozone, *J. Geophys. Res.*, this issue.

Donahue, N. M., and R. G. Prinn, In situ nonmethane hydrocarbon measurements on SAGA 3, *J. Geophys. Res.*, *98*, 16,915–16,932, 1993.

Fishman, J., S. Solomon, and P. J. Crutzen, Observational and theoretical evidence in support of a significant in-situ source of tropospheric ozone, *Tellus*, *31*, 432–446, 1979.

Gregory, G. L., A. S. Bachmeier, D. R. Blake, B. G. Heikes, D. C. Thornton, A. R. Bandy, J. D. Bradshaw, and Y. Kondo, Chemical signatures of aged Pacific marine air: Mixed layer and free troposphere as measured during PEM-West A, *J. Geophys. Res.*, this issue.

Heikes, B. G., Formaldehyde and hydroperoxides at Mauna Loa Observatory, *J. Geophys. Res.*, *97*, 18,001–18,013, 1992.

Heikes, B. G., and B. Mosher, Hydrogen peroxide and methylhydroperoxide during SAGA-III (abstract), *Eos Trans. AGU*, *71*, 1230, 1990.

Heikes, B. G., G. L. Kok, J. G. Walega, and A. L. Lazrus, H_2O_2, O_3, and SO_2 measurements in the lower troposphere over the eastern United States during the fall., *J. Geophys. Res.*, *92*, 915–931, 1987.

Heikes, B. G., B. McCully, G. L. Kok, and T. Staffelbach, Seasonal variation in H_2O_2, CH_3OOH, and CH_2O during MLOPEX-II (abstract), *Eos Trans. AGU*, *74*, p. 119, 1993.

Heikes, B. G., et al., Ozone, hydroperoxides, oxides of nitrogen, and hydrocarbon budgets in the marine boundary layer over the South Atlantic, *J. Geophys. Res.*, in press, 1995.

Hirsch, R. M., and E. J. Gilroy, Methods of fitting a straight line to data: Examples in water resources, *Water Resour. Bull.*, *20*, 705–711, 1984.

Hoell, J. M., D. D. Davis, S. C. Liu, R. Newell, M. Shipham, H. Akimoto, R. J. McNeal, R. J. Bendura, and J. W. Drewry, Pacific Exploratory Mission-West A (PEM-West A): September–October 1991, *J. Geophys. Res.*, this issue.

Hubler, G., et al., Total reactive oxidized nitrogen (NO_y) in the remote Pacific troposphere and its correlation with O_3 and CO: Mauna Loa Observatory photochemistry experiment, *J. Geophys. Res.*, *97*, 10,427–10,447, 1992.

Jacob, D. J., S. Sillman, J. A. Logan, and S. C. Wofsy, Least independent variable method for simulation of tropospheric ozone, *J. Geophys. Res.*, *94*, 8497–8509, 1989.

Jacob, D. J., J. A. Logan, G. M. Gardner, R. M. Yevich, C. M. Spivakovsky, S. C. Wofsy, S. Sillman, and M. J. Prather, Factors regulating ozone over the United States and its export to the global atmosphere, *J. Geophys. Res.*, *98*, 14,817–14,826, 1993.

Jacob, D. J., L. W. Horowitz, B. G. Heikes, R. R. Dickerson, R. S. Artz, and W. C. Keene, Seasonal transition from NO_x-to hydrocarbon-limited ozone production over the eastern United States in early fall, *J. Geophys. Res.*, *100*, 9315–9324, 1995.

Kleinman, L. I., Seasonal dependence of boundary layer peroxide concentrations: The low and high NO_x regimes, *J. Geophys. Res.*, *96*, 20,721–20,733, 1990.

Koike, M., Y. Kondo, S. Kawakami, H. B. Singh, H. Ziereis, and J. T. Merrill, Ratios of reactive nitrogen species over the Pacific during PEM-West A, *J. Geophys. Res.*, this issue.

Kondo, Y., H. Ziereis, M. Koike, S. Kawakami, G. L. Gregory, G. W. Sachse, H. B. Singh, D. D. Davis, and J. T. Merrill, Reactive nitrogen over the Pacific Ocean during PEM-West A, *J. Geophys. Res.*, this issue.

Kriedenweis, S. M., and J. H. Seinfeld, Nucleation of sulfuric acid-water and methanesulfonic acid-water solution particles: Implications for the atmospheric chemistry of organosulfur compounds, *Atmos. Environ.*, *22*, 283–296, 1988.

Lazrus, A. L., G. L. Kok, J. A. Lind, S. N. Gitlin, B. G. Heikes, and R. E. Shetter, Automated fluorometric determination of hydrogen peroxide vapor in air, *Anal. Chem.*, *58*, 5594–5597, 1986.

Lee, J., D. F. Leahy, I. N. Tang, and L. Newman, Measurement and speciation of gas phase peroxides in the atmosphere, *J. Geophys. Res.*, *98*, 291–2915, 1993.

Lee, M., Hydrogen peroxide, methylhydroperoxide and formaldehyde in air impacted by biomass burning, Ph.D. dissertation, Univ. of Rhode Island, Narragansett, R. I., 1995.

Lee, M., D. O'Sullivan, K. B. Noone, and B. G. Heikes, HPLC method for the determination of H_2O_2, C1, and C2 hydroperoxides in the atmosphere, *J. Atmos. Oceanic Technol.*, *12*, 1060–1070, 1995.

Lee, R. N., and K. M. Busness, The concentration and vertical distribution of peroxides over the Pacific Ocean during the Pacific Stratus Investigation (abstract), *Eos Trans. AGU*, *70*, 1030, 1989.

Leighton, P. A., *Photochemistry of Air Pollution*, Academic, San Diego, Calif., 1961.

Levy, H., Photochemistry of minor constituents of the troposphere, *Planet. Space Sci.*, *21*, 575–591, 1973.

Lin, X. M., M. Trainer, and S. C. Liu, On the nonlinearity of tropospheric ozone production, *J. Geophys. Res.*, *93*, 15,879–15,888, 1988.

Lind, J. A., and G. L. Kok, Henry's law determinations of hydrogen peroxide, methylhydroperoxide, and peroxyacetic acid, *J. Geophys. Res.*, *91*, 7889–7895, 1986.

Lind, J. A., and G. L. Kok, Correction to "Henry's law determinations of hydrogen peroxide, methylhydroperoxide, and peroxyacetic acid, *J. Geophys. Res.*, *99*, 21,119, 1994.

Lind, J. A., B. G. Heikes, G. L. Kok, and A. L. Lazrus, Tropospheric measurements of H_2O_2, O_3, and CH_2O over the Pacific Ocean in January (abstract), *Eos Trans. AGU*, *68*, 1212, 1987.

Liu, S. C., et al., A study of the photochemistry and ozone budget during the Mauna Loa Observatory photochemistry experiment, *J. Geophys. Res.*, 10,463–10,471, 1992.

Liu, S. C., et al., Model study of tropospheric trace species distributions during PEM-West A, *J. Geophys. Res.*, this issue.

Logan, J. A., M. J. Prather, S. C. Wofsy, and M. B. McElroy, Tropospheric chemistry: A global perspective, *J. Geophys. Res.*, *86*, 7210–7254, 1981.

McKeen, S. A., et al., Hydrocarbon ratios during PEM-West A: A model perspective, *J. Geophys. Res.*, this issue.

Merrill, J. T., Trajectory results and interpretation for PEM-West A, *J. Geophys. Res.*, this issue.

Miller, W., An investigation of peroxide, iron, and iron bioavailability in irradiated marine waters, Ph.D. thesis, Univ. of Rhode Island, Narragansett, 1990.

National Center for Atmospheric Research (NCAR), NCAR-ADMP, ADMP-86-4, Preliminary evaluation studies with the regional acid deposition model (RADM), *NCAR Tech. Note*, *NCAR/TN-265+STR*, Boulder, Colo., 1986.

National Research Council (NRC), *Tropospheric Chemistry: A Plan for Action*, Natl. Acad. Press, Washington, D. C., 1984.

Newell, R. E., et al., Atmospheric sampling of supertyphoon Mireille with the NASA DC-8 aircraft on September 27, 1991, during PEM-West A, *J. Geophys. Res.*, this issue (a).

Newell, R. E., et al., Potential vorticity and stratospheric/tropospheric exchange: One pilot study with applications to PEM-West A, *J. Geophys. Res.*, this issue (b).

Norton, R. B., M. A. Carroll, D. D. Montzka, G. Hubler, B. J. Huebert, G. Lee, W. Warren, B. A. Ridley, and J. G. Walega, Measurements of nitric acid and aerosol nitrate at the Mauna Loa Observatory during the Mauna Loa Observatory Photochemistry Experiment 1988, *J. Geophys. Res.*, 10,415–10,425, 1992.

O'Sullivan, D., M. Lee, K. B. Noone, and B. G. Heikes, Henry's law solubility of hydrogen peroxide, methylhydroperoxide, hydroxymethylhydroperoxide, 1-hydroxy-ethylhydroperoxide, peroxyacetic acid and ethylhydroperoxide, *J. Phys. Chem.*, in press, 1995.

Parrish, D. D., M. Trainer, E. J. Williams, D. W. Fahey, G. Hubler, C. S. Eubank, S. Liu, P. C. Murphy, D. L. Albritton, and F. C. Fehsenfeld, *J. Geophys. Res.*, *9*, 5361–5370, 1986.

Penkett, S. A., B. M. R. Jones, K. A. Brice, and A. E. J. Eggleton, The importance of atmospheric ozone and hydrogen peroxide in oxidizing sulfur dioxide in cloud and rain water, *Atmos. Environ.*, *13*, 123–137, 1978.

Ridley, B. A., S. Madronich, R. B. Chatfield, J. G. Walega, and R. E. Shetter, Measurements and model simulations of the photostationary state during the Mauna Loa Observatory photochemistry experiment: Implications for radical concentrations and ozone loss rates, *J. Geophys. Res.*, *97*, 10,375–10,388, 1992.

Smyth, J., et al., Comparison of free tropospheric western Pacific air mass classification schemes for the PEM-West A experiment, *J. Geophys. Res.*, this issue.

Stedman, D. H., and J. O. Jackson, The photostationary state in photochemical smog, *Int., J. Chem. Kinet. Symp.*, *1*, 493–501, 1975.

Talbot, R. W., et al., Chemical characteristics of continental outflow from Asia to the troposphere over the western Pacific Ocean during September–October 1991: Results from PEM-West A, *J. Geophys. Res.*, this issue.

Thompson, A. M., et al., Ozone observations and a model of marine boundary layer photochemistry during SAGA 3, *J. Geophys. Res.*, *98*, 16,955–16,968, 1993.

Thornton, D. C., et al., Sulfur dioxide as a source of CN in the upper troposphere of the Pacific Ocean, *J. Geophys. Res.*, this issue.

Trainer, M., E. J. Williams, D. D. Parrish, M. P. Buhr, E. J. Allwine, H. H. Westberg, F. C. Fehsenfeld, and S. C. Liu, Models and observations of the impact of natural hydrocarbons on rural ozone, *Nature*, *329*, 705–707, 1987.

Van Valin, C. C., M. Luria, J. D. Ray, and J. F. Boatman, A comparison of surface and airborne trace gas measurements at a rural Pennsylvania site, *J. Geophys. Res.*, *97*, 20,745–20,754, 1991.

Wang, C., and J. S. Chang, A three-dimensional numerical model of cloud dynamics, microphysics, and chemistry, 3, Redistribution of pollutants, *J. Geophys. Res.*, *98*, 16,787–16,798, 1993a.

Wang, C., and J. S. Chang, A three-dimensional numerical model of cloud dynamics, microphysics, and chemistry, 4, Cloud chemistry and precipitation chemistry, *J. Geophys. Res.*, *98*, 16,799–16,808, 1993b.

A. Bandy and D. Thornton, Drexel University, Philadelphia, PA 19104.

D. Blake, University of California, Irvine, CA 92717.

J. Bradshaw, J. Crawford, D. D. Davis and S. Sandholm, Georgia Institute of Technology, Atlanta, GA 30332.

G. Gregory, NASA Langley Research Center, Hampton, VA 23681.

B. G. Heikes (corresponding author) and M. Lee, Center for Atmospheric Chemistry Studies, Graduate School of Oceanography, University of Rhode Island, Narragansett, RI 02882-1197.

S. Liu, NOAA Aeronomy Laboratory, 325 Broadway, Boulder, CO 80303.

S. McKeen, NOAA Cooperative Institute for Research in Environmental Sciences, Boulder, CO 80303.

J. Rodriguez, AER Inc., 840 Memorial Drive, Cambridge, MA 02139.

R. Talbot, Institute for the Study of Earth, Oceans, and Space, University of New Hampshire, Durham, NH 03824.

(Received February 11, 1994; revised March 26, 1995;
accepted March 26, 1995.)